ELECTROSTATIC CALCULATIONS FOR AN ION CHANNEL

II. KINETIC BEHAVIOR OF THE GRAMICIDIN A CHANNEL

DAVID G. LEVITT, *Department of Physiology, University of Minnesota, Minneapolis, Minnesota 55455 U.S.A.*

ABSTRACT A theoretical model of the gramicidin A channel is presented and the kinetic behavior of the model is derived and compared with previous experimental results. The major assumption of the model is that the only interaction between ions in a multiply-occupied channel is electrostatic. The electrostatic calculations indicate that there will be potential wells at each end of the channel and, at high concentrations, that both wells can be occupied. The kinetics are based on two reaction steps: movement of the ion from the bulk solution to the well and movement between the two wells. The kinetics for this reaction rate approach are identical to those based on the Nernst-Planck equation in the limit where the movement between the two wells is rate limiting. The experimental results for sodium and potassium are consistent with a maximum of two ions per channel. To explain the thallium results it is necessary to allow three ions per channel. It is shown that this case is compatible with the electrostatic calculations if the presence of an anion is included. The theoretical kinetics are in reasonable quantitative agreement with the following experimental measurements: single channel conductance of sodium, potassium, and thallium; bi-ionic potential and permeability ratio between sodium-potassium and potassium-thallium; the limiting conductance of potassium and thallium at high applied voltages; current-voltage curves for sodium and potassium at low (but not high) concentrations; and the inhibition of sodium conductance by thallium. The results suggest that the potential well is located close to the channel mouth and that the conductance is partially limited by the rate of going from the bulk solution to the well. For thallium, this entrance rate is probably diffusion limited.

INTRODUCTION

In the first paper (Levitt, 1978) it was shown how the electrostatic energy profile of an ion in a membrane channel could be calculated. The most important aspect of these calculations is that they can be used to determine the electrostatic interaction between ions if there is more than one ion per channel. Because it is probable that the dominant interaction is electrostatic, these calculations can be used to predict the kinetic behavior of multiply occupied channels. The purpose of this paper is to examine the theoretical behavior of multiply-occupied channels on the basis of the assumption that the only interaction between ions is electrostatic. These theoretical results will then

BIOPHYS. J. © Biophysical Society · 0006-3495/78/0501-221 $1.00

be compared with the experimental conductance and bi-ionic potential data for the gramicidin channel.

It is now apparent that the kinetic behavior of the gramicidin channel is complicated. The clearest indication of this complexity is demonstrated by the behavior of thallium. Thallium has a single channel conductance vs. concentration curve similar to potassium and sodium, reaching a maximum conductance at concentrations of about 1 M. If it is assumed that there is at most one ion per channel than it can be shown from a rather general model that thallium should have an affinity constant in the channel of about 0.3 M (Läuger, 1973). However, Neher (1975) found that very low thallium concentrations (2 mM) could partially block the sodium conductance. This strongly suggests that thallium must also have a high affinity site either in or very near the pore and that at high concentrations at least two ions per channel must be involved. Recently, Eisenman et al. (1976) and Sandblom et al. (1977) have carried out detailed investigations of the kinetic behavior of thallium and potassium in the gramicidin channel. They have confirmed the previous results and pointed out some new complexities. To explain these results, they have proposed a rather complicated model that involves four binding sites (two at each end). They assumed that the exchange between the binding sites and the bulk water was fast and that the rate-limiting step was an energy barrier in the center of the membrane. If the size of this barrier were arbitrarily varied as a function of the number of sites occupied and the type of ion, then most of the experimental observations could be explained. It will be shown in this paper that these data can be equally well explained by a simple physical model in which only electrostatic interactions between ions are assumed.

Recently, Hladky et al. (1978) have examined the Na^+ and K^+ experimental results for gramicidin with a model similar to the one proposed here. Also, a similar type of model has been used previously in analyses of the theoretical behavior of the sodium channel (Heckman et al., 1972; Hille, 1975*a*; and Chizmadjev and Aityan, 1977).

The kinetic description is based on the free energy diagram shown in Fig. 1: $U(x)$ is a qualitative estimate of the local free energy of interaction between the ion and the wall (relative to the bulk solution) and $E(x)$ is the electrostatic energy calculated in the first paper (Levitt, 1978) for a pore that contains one ion. The energy is in units of $kT\,(T = 300°\text{K})$. It can be seen that there is a well or minimum in the total energy profile $(E + U)$ where there should be a high probability of finding the ion. The exact position of this well depends on the shape of $U(x)$ but it should be near the pore ends. Unless otherwise noted, it will be assumed that the well is 1 Å from each end. The kinetics for this system can be generally described in terms of two reaction steps. The first is the movement between the bulk solution and the well. This reaction may be limited by the rate of partial dehydration or exchange with water or it may be diffusion-limited. The second reaction is the movement across the membrane from one well to the other. This rate is determined by the size of the energy barrier and the local mobility in the channel. The wiggles in the $U(x)$ line represent the local free energy barrier encountered by the ion as it moves from one binding site to the next in the pore. The size of these wiggles determines the local mobility.

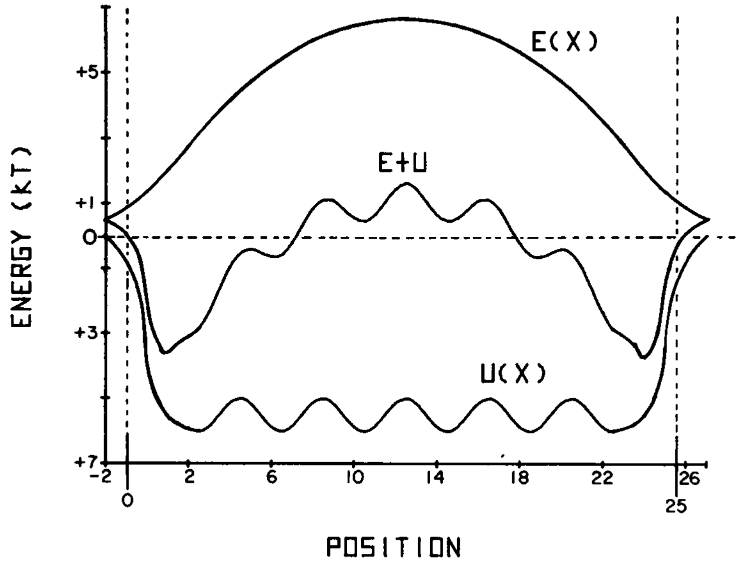

FIGURE 1 Local free energy of interaction between ion and channel wall relative to bulk solution (U), electrostatic energy (E), and total energy ($E + U$) as a function of distance of ion from left end of channel. The dashed lines indicate the position of channel ends.

It was shown in the first paper that the interaction between the first two ions in the channel may be small so that one would expect to find two ions per channel at high bulk concentrations. The kinetics for the case where there is a maximum of two ions per channel will be examined in section I. It will be shown that the conductance and bi-ionic potential data for sodium and potassium can be satisfactorily described by this case. To explain the thallium results it is necessary to consider the case where there is a maximum of three ions per channel. This case will be examined in section II.

I. *Maximum of Two Ions Per Channel (Sodium and Potassium)*

A useful way to describe the model is in terms of the following state diagram (for the case where there is only a single cation present with activities c_1 and c_2 in the left- and right-hand solutions, respectively):

(I)

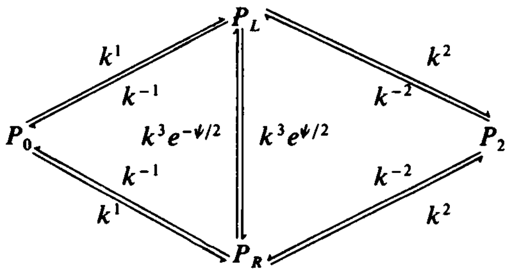

The channel can be in four different states with probability P: empty of cations (P_0); an ion in the left well (P_L); an ion in the right well (P_R); and both wells occupied

(P_2). The kinetics are determined by the transition probabilities between the different states. For example, the probability of going from P_0 to P_L is $c_1k^1P_0$; and from P_L to P_R is $k^3 \exp(\psi/2)$, where k^1 and k^3 are specific rate constants and ψ ($= F\psi/RT$) is the dimensionless potential across the membrane. Hladky et al. (1978) have assumed in their model that the entrance (k^1) and exit (k^{-1}) steps are also potential dependent. This adds several additional variables to a model that already has an excess of adjustable parameters. In this paper, it will be assumed, as a first approximation, that the wells are so close to the ends of the channel that there is no significant potential difference between the well and the bulk solution, so that the only step that is potential-dependent is the rate of crossing the membrane. This is a reasonable assumption because one would expect the well to be within 1 or 2 Å of the channel end because of the steep rise of the electrostatic barrier (Fig. 1). Following the usual procedure in reaction rate theory, the rate in the presence of the applied potential has been written in terms of the rate in the absence of the potential (k^3) times the exponential of the difference in the applied potential between the peak of the barrier in the center of the membrane ($\psi/2$) and the well (≈ 0). (It was shown in the first paper that the applied potential gradient in the pore was linear.) A more physical approach can be used if the reaction at the channel ends is very fast compared with the rate of crossing the membrane. Then, the kinetics can be derived from the Nernst-Planck equation by assuming that the ion at the end stays in equilibrium with the bulk solution as the other ion crosses the membrane. This limit is analyzed in the Appendix, and it is shown that even though the ends are in equilibrium, there is still interaction between ions if the channel is multiply occupied. This approach has not been examined further because the experiments indicate that there is partial limitation at the channel ends.

The ion flux through the channel in diagram I is:

$$J = k^3(P_Le^{\psi/2} - P_Re^{-\psi/2}). \tag{1}$$

This equation assumes that the ion can only cross the membrane if the other well is unoccupied. This means that although the probability of jumping across the membrane may be low, when an ion does jump its velocity is fast compared with the rate of leaving the channel end. Otherwise, it would be necessary to allow the movement of the ion across the membrane to displace the ion at the other end. The flux is obtained by solving the state diagram for the probability of being in the different states and then substituting into Eq. 1.

CHANNEL CONDUCTANCE The conductance is measured with identical solutions on both sides of the membrane ($c_1 = c_2 = c$). The final expression for the flux for this case is (see Appendix, Eq. 4A ($k^6 = k^2, k^{-6} = k^{-2}$) and Eq. 6A):

$$J = \frac{ck^3(k^{-1} + ak^2)(e^{\psi/2} - e^{-\psi/2})}{[k^{-1} + k^3(e^{\psi/2} + e^{-\psi/2}) + ak^2](K_1 + 2a + a^2/K_2)};$$

$$K_1 = k^{-1}/k^1; K_2 = k^{-2}/k^2, \tag{2}$$

where K_1 and K_2 are the dissociation constants for the first and second ion. In this section only the concentration dependence of the conductance will be examined, and it will be assumed that the measurements were made in the limit of zero-applied potential. This assumption is valid because the experiments were made in a potential range where the conductance did not differ significantly from this limit (Hladky and Haydon, 1972).

Because there are five adjustable parameters in Eq. 2, it is not surprising that the experimental data can be fit. However, the range of the allowed values becomes much more limited when the conductance results are combined with the results from other experiments (see below). One of the parameters will be removed by assuming that the difference between the two equilibrium constants K_1 and K_2 is due entirely to the difference in the rate of entering the channel:

$$K_1/K_2 = k^2/k^1. \tag{3}$$

This is an arbitrary assumption made to simplify the analysis. The data can be fit just as well if it is assumed that the exit and entrance steps are symmetrically affected by the second ion. With this assumption, the conductance can be written in dimensionless form in terms of two parameters (in the limit of zero potential):

$$\begin{aligned} G' &= (RT/F^2)G^0/k^3 = \lim_{\psi \to 0} J/(k^3\psi);\ c' = c/K_1, A = K_2/K_1 \\ &= \frac{c'}{[1 + 2/(B + Bc'/A)][1 + 2c' + c'^2/A]};\ B = k^{-1}/k^3, \end{aligned} \tag{4}$$

where G' and c' are the dimensionless conductance and concentration. The parameters k^3 and K_1 determine the absolute scaling and A and B determine the shape of the conductance vs. concentration curve.

The value of $A(K_2/K_1)$ can be estimated from the electrostatic energy calculation. The dissociation constant for the binding of the first (K_1) and the second (K_2) ions is equal to:

$$K_1 = \exp(U + E_1);\ K_2 = \exp(U + E_2 - E_1), \tag{5}$$

where U is the local free energy of interaction with the wall and E_1 and E_2 are the electrostatic energies (relative to the bulk solution) for a pore that contains one or two ions. It has been assumed that since U is a local energy, it does not depend on the num-

TABLE I

CALCULATION OF K_2/K_1 FROM ELECTROSTATIC ENERGY (kt)

Distance from channel end	E_1 (1 ion)	E_2 (2 ions)	E_i^2 $(E_2 - 2E_1)$	K_2/K_1 (Eq. 6)
(Å)				
0	1.361	3.313	0.591	1.806
1	2.03	5.02	0.96	2.61
2	2.79	7.059	1.48	4.39
3	3.525	9.193	2.14	8.52

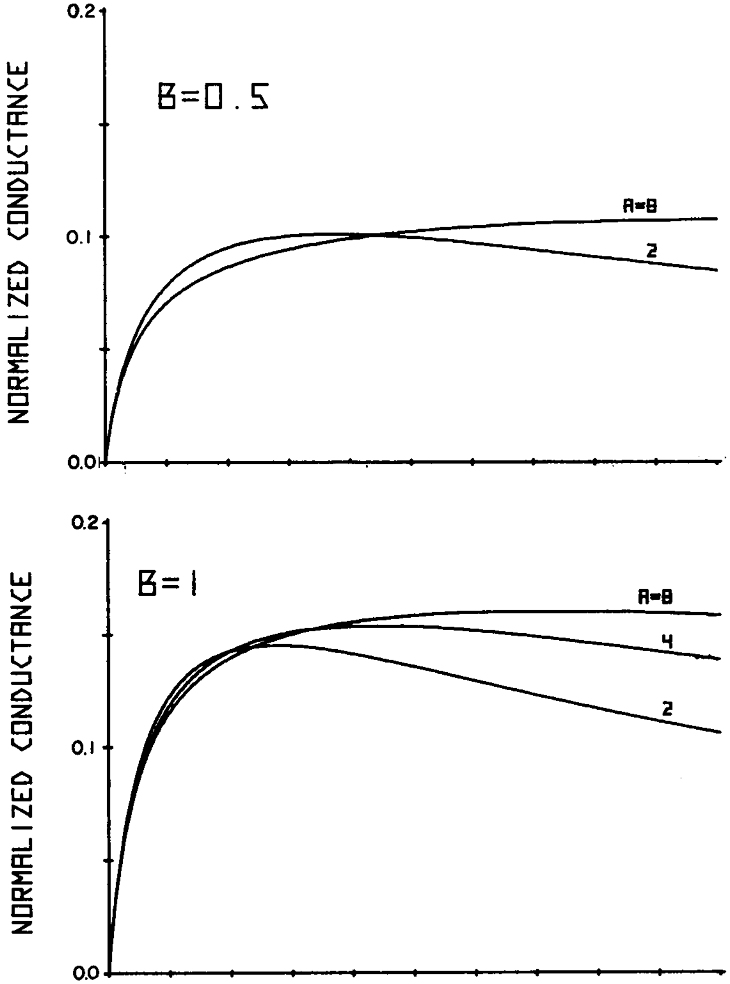

FIGURE 2 Normalized channel conductance (Eq. 4) for B varying from 0.5 to 6 and A varying from 2 to 8.

ber of ions in the pore. The ratio of the dissociation constants is:

$$A = K_2/K_1 = \exp(E_i^2); \qquad E_i^2 = E_2 - 2E_1. \tag{6}$$

The values of E_1 and E_2 determined by the procedure described in the first paper are listed in Table I as a function of the distance of the well from the end of the channel. The value of the interaction energy (E_i^2) is listed in the third column, and the ratio of the dissociation constants (A) is listed in the fourth column. It can be seen that the minimum value of A is about 2. Also, because it is unlikely that the well is more than about 3 Å into the channel (see below), the maximum value of A is about 8.

Eq. 4 is plotted in Fig. 2 for this range of A and for B varying from 0.5–6. The gen-

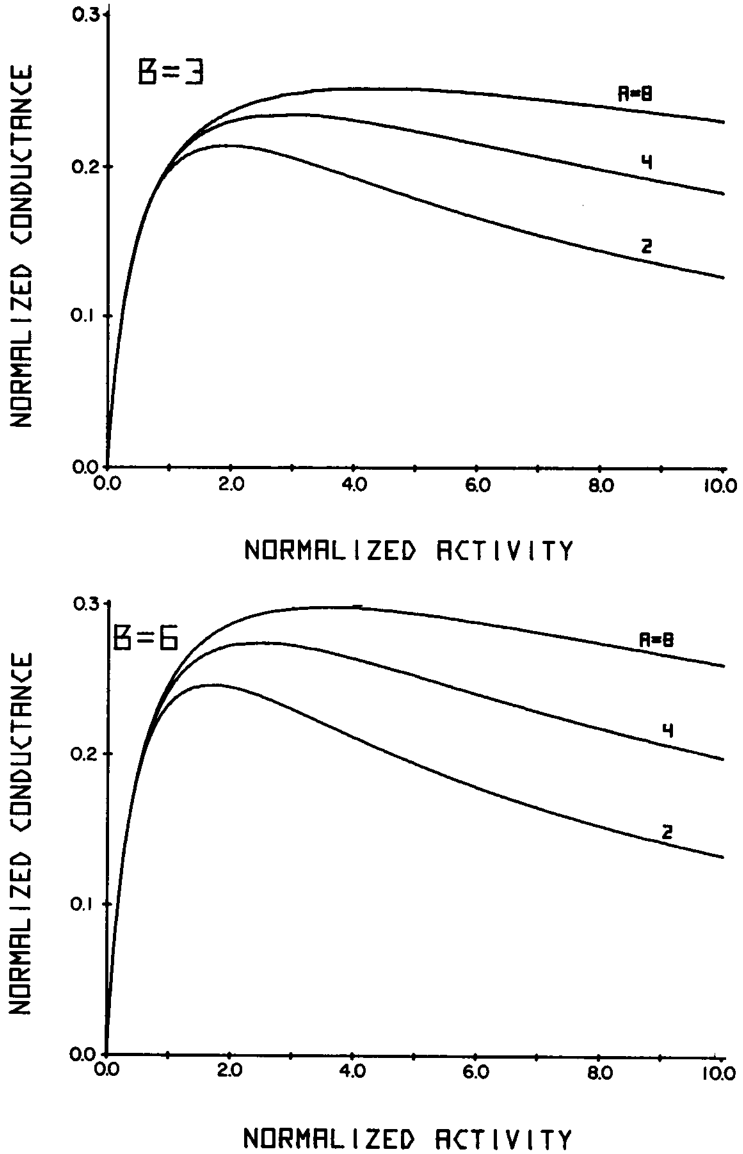

FIGURE 2 (*continued*)

eral shape of the sodium and potassium conductance can be described by a number of different combinations of A and B. However, the voltage dependence of the conductance (see below) indicates that B should be about 1. Varying B around 1, a satisfactory fit was found for potassium ($A = 2$, $B = 1$) and sodium ($A = 8$, $B = 2$). From the absolute values of the experimental data, one can determine the scaling factors k^3 (and then $k^{-1} = Bk^3$) and K_1 (and then $k^1 = k^{-1}/K_1$ and $K_2 = AK_1$). The constants determined from these conductance measurements and from the other experimental

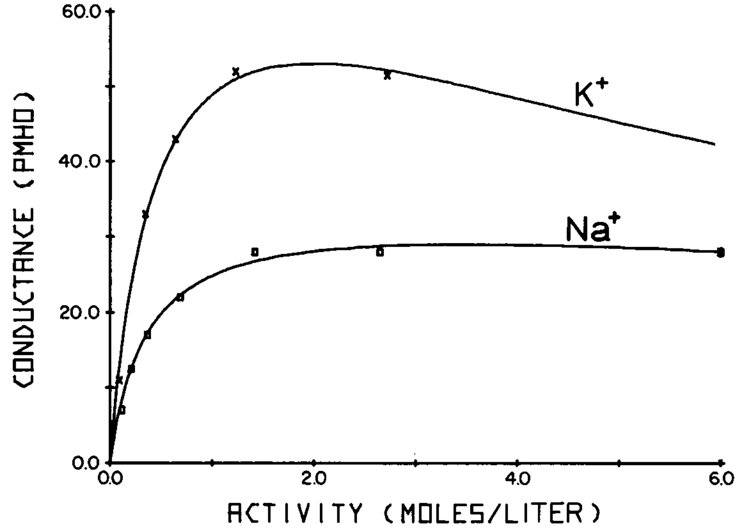

FIGURE 3 Theoretical single channel conductance curves (solid lines) for potassium ($A = 2$, $B = 1$), sodium ($A = 8$, $B = 2$), and experimental data (x, □) from Hladky (1974).

procedures are summarized in Table V. An independent test of the theory is provided by the fact that the k^1 for potassium determined above (1.34×10^{-16} liters/s) is in good agreement with the value determined directly by Andersen (1978) from the limiting conductance at high applied voltages (1.5×10^{-16}). These theoretical conductance curves are plotted in Fig. 3 along with the experimental data of Hladky (1974). Although the theory provides a satisfactory fit to the general shape of the experimental curves, it does miss some of the fine structure. In particular, the sodium curve does not peak soon enough and the theoretical value of the ratio of the potassium to sodium conductance in the limit of zero concentration is 1.9 compared with the experimental value of about 2.5. Some of this discrepancy may be the result of experimental errors, especially in the low concentration, low conductance range.

BI-IONIC POTENTIAL Myers and Haydon (1972) measured the membrane potential (ψ_T) when potassium (b) was on the left side of the membrane and an equal concentration of sodium (c) was on the right side. The potential was related to a permeability ratio by the Goldman equation:

$$\exp(\psi_T) = P_c/P_b. \tag{7}$$

The system is described by the following state diagram when there are two different ions present:

(II)

$$\begin{tikzcd}
 & & P^c_2 \arrow[dl, shift left] \arrow[dl, leftarrow, shift right] \arrow[dr, shift left] \arrow[dr, leftarrow, shift right] & & \\
 & P^c_R \arrow[rr, shift left] \arrow[rr, leftarrow, shift right] \arrow[dl, shift left] \arrow[dl, leftarrow, shift right] \arrow[dr, shift left] \arrow[dr, leftarrow, shift right] & & P^c_L \arrow[dl, shift left] \arrow[dl, leftarrow, shift right] \arrow[dr, shift left] \arrow[dr, leftarrow, shift right] & \\
P_{bc} \arrow[dr, shift left] \arrow[dr, leftarrow, shift right] & & P_0 \arrow[dl, shift left] \arrow[dl, leftarrow, shift right] \arrow[dr, shift left] \arrow[dr, leftarrow, shift right] & & P_{cb} \arrow[dl, shift left] \arrow[dl, leftarrow, shift right] \\
 & P^b_L \arrow[rr, shift left] \arrow[rr, leftarrow, shift right] \arrow[dr, shift left] \arrow[dr, leftarrow, shift right] & & P^b_R \arrow[dl, shift left] \arrow[dl, leftarrow, shift right] & \\
 & & P^b_2 & &
\end{tikzcd}$$

The general solution for this diagram is very complicated and will not be attempted here. However, as a first approximation it will be assumed that the net flux of ions through P_{bc} and P_{cb} is negligible. This assumption is reasonable because, first, P_{bc} is small because P_2 is small for sodium ($K_2/K_1 \approx 8$) and P_{bc} should be intermediate between $P_2$for sodium and potassium. Secondly, even if P_{bc} were not small, the fluxes in the two directions should be approximately equal. With this assumption, the flux of b and c become coupled only through P_0 and the solute flux for the case where $[\mathrm{K}]_1 = a, [\mathrm{K}]_2 = 0, [\mathrm{Na}]_1 = 0, [\mathrm{Na}]_2 = a$ can be written in the form (see Appendix, Eq. 11A):

$$J_{\pm} = \pm \frac{ak^1k^3(ak^2 + 2k^{-1})\, e^{\pm\psi/2}}{k^{-1}[ak^2 + 2k^{-1} + 2k^3(e^{\psi/2} + e^{-\psi/2})]} P_0, \tag{8}$$

where the plus is for the ion on the left side and the minus is for the ion on the right side. The bi-ionic condition is:

$$J_b + J_c = 0. \tag{9}$$

Substituting Eq. 8 into Eq. 9:

$$e^{-\psi} = P_b/P_c = \frac{k_b^3K_1^c[1 + (e^{\psi/2} + e^{-\psi/2})k_c^3/(k_c^{-1} + 0.5a\, k_c^2)]}{k_c^3K_1^b[1 + (e^{\psi/2} + e^{-\psi/2})k_b^3/(k_b^{-1} + 0.5a\, k_b^2)]}. \tag{10}$$

It can be seen that the permeability ratio (defined by Eq. 7) is voltage-dependent. If the rate of leaving the channel end (k^{-1}) is fast compared with the rate of crossing the membrane (k^3) then the permeability ratio will be a constant, independent of concentration. This is consistent with the result (see Appendix) that the permeability ratio derived from the Nernst-Planck equation (assuming equilibrium at the ends) is independent of concentration. This analysis implies that under rather general conditions, a concentration dependence of the permeability ratio indicates some rate limitation at the ends of the channel if the only interaction between ions is electrostatic. The permeability ratio can be written in terms of the ratio in the limit of zero concentration $(P_b/P_c)_0$ and the parameters A, B, and K_1:

$$\frac{P_b/P_c}{(P_b/P_c)_0} = \left[\frac{1 + (e^{\psi/2} + e^{-\psi/2})/(1 + 0.5a/K_1^cA_c)B_c}{1 + (e^{\psi/2} + e^{-\psi/2})/B_c}\right] \cdot \left[\frac{1 + (e^{\psi/2} + e^{-\psi/2})/B_b}{1 + (e^{\psi/2} + e^{-\psi/2})/(1 + 0.5a/K_1^bA_b)B_b}\right]. \tag{11}$$

This ratio is listed in Table II as a function of concentration for the values of the parameters used in Fig. 3 (Table V) and using the experimentally observed value of ψ (1.4). The experimental results of Myers and Haydon (1972) are also listed, and it can be seen that the agreement is good. The permeability ratio can only be fit by a very limited range of values. For example, B for potassium must be less than about 2 and the A for sodium must be several times larger than the A for potassium.

TABLE II

PERMEABILITY RATIO FROM BI-IONIC POTENTIAL FOR K^+ AND Na^+

Concentration	$(P_K/P_{Na})/(P_K/P_{Na})_0$	
	Experimental*	Theoretical‡
(mol/liter)		
10^{-3}	1.0	1
10^{-2}	1.0	1.00
10^{-1}	1.0	1.02
1	1.13	1.17
3	1.32	1.38
5	—	1.51
10	—	1.65

*Myers and Haydon, 1972.
‡Eq. 11.

It can be seen by comparing Eqs. 4 and 10 that, in the limit of zero concentration and potential, the permeability ratio should equal the conductance ratio. This equality is a general result and it should hold for a larger class of models than was assumed here (Hille, 1975*b*). Thus, it is difficult to explain the experimental observation that the limiting conductance ratio is 2.5 whereas the permeability ratio is 3.3 (Myers and Haydon, 1972). Hladky et al. (1978) suggest that this inequality indicates that the channel is multiply occupied with K^+ and Na^+ at the lowest concentrations for which the ratio was measured (10 mM). However, this would be difficult to reconcile with the conductance measurements of Eisenman et al. (1976) and would imply that the gramicidin channel had a surprisingly high affinity for Na^+ and K^+. Hladky et al. (1978) also point out that there may be errors in the absolute values of the conductance at low activities and that this discrepancy may be due to experimental errors.

POTENTIAL DEPENDENCE OF THE CONDUCTANCE Hladky and Haydon (1972) have shown that the sodium and potassium current vs. voltage plots have a complicated concentration dependence: bending toward the voltage axis at low concentrations and toward the current axis at high concentrations. Andersen (1978) has extended these measurements and determined the limiting conductance at high potentials. The potential dependent part of the flux (Eq. 2) is (assuming Eq. 3):

$$I = \frac{e^{\psi/2} - e^{-\psi/2}}{e^{\psi/2} + e^{-\psi/2} + B(1 + a/AK_1)}. \qquad (12)$$

At low concentrations, the shape of the *I-V* curve is determined entirely by B. As was mentioned above, in order to fit the experimental *I-V* curves for sodium and potassium at low concentrations, B should be about 1 or 2. Eq. 12 is plotted in Fig. 4 for the parameters that were used for potassium ($A = 2$, $B = 1$, $K_1 = 0.73$ M). The abscissa is labeled in units of ψ and the equivalent transmembrane potential ($\Psi = RT\psi/F$). Qualitatively, Eq. 12 has the correct potential dependence, bending toward the voltage

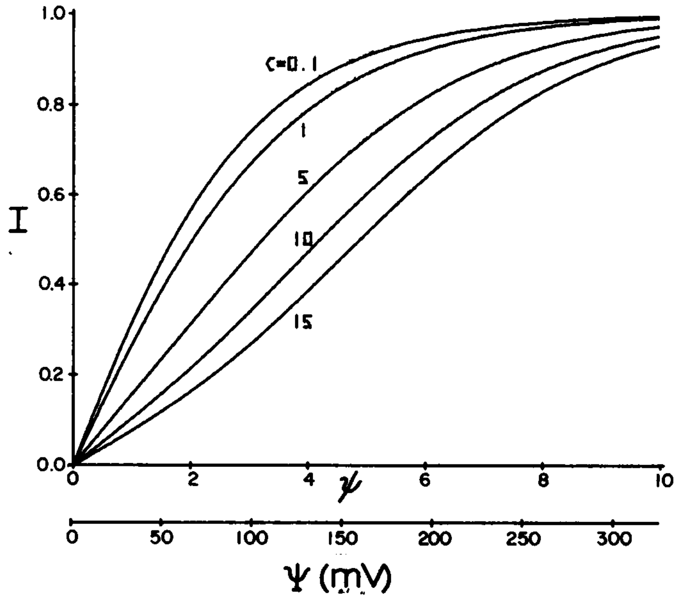

FIGURE 4 Potassium current (I, Eq. 12) as a function of either the dimensionless potential difference (ψ) or the absolute potential drop across the whole membrane ($\psi = F\Psi_T/RT$) for potassium activity (c) varying from 0.1 to 15 M.

axis for concentrations less than about 5 M/liter, and bending toward the current axis (for Ψ < 150 mV) for concentrations >5 M. Quantitatively, however, the agreement between theory and experiment is not very good. The experimental curves are nearly straight for concentrations of 0.5 and 1 M whereas the theoretical curves are still curved. The discrepancy is more serious for sodium, which has the low concentrations shape at nearly all concentrations, because of the large value of A needed to fit the other data. This inability of the theory to explain the current-voltage curves at high concentrations is probably due in part to the neglect of the potential dependence of the exit and entrance steps. In addition, at high applied potentials, the voltage drop in the bulk solutions becomes significant (Läuger, 1976), and this has also been neglected.

II. *Maximum of Three Ions per Channel (Thallium)*

THALLIUM CONDUCTANCE Measurements of the single channel conductance as a function of thallium concentration show that the conductance can be described by Michaelis-Menten type kinetics with two apparent binding sites (Eisenman et al. 1976). At low concentrations, the gramicidin channel has an apparently high affinity ($K_m \simeq$ 1 mM) and low maximum conductance ($V_m \simeq$ 2.2 pmho). At high concentrations, the channel has a low affinity ($K_m \simeq$ 80 mM) and high V_m (48 pmho).

In the low concentration range there should be at most two ions per channel so that the experimental conductance data should be described by the same model (Eq. 4) used for Na^+ and K^+, differing only in that the dissociation constants K_1 and K_2 are much smaller. As was discussed above, even with the detailed data available for sodium and potassium, it was not possible to determine uniquely the theoretical constants from the conductance data. The case is worse for thallium because what would correspond to the high concentration portion of the conductance curve is obscured by the low affinity component. However, it will be shown that the thallium conductance is probably diffusion limited and therefore the rate-limiting step is at the channel end and, to a first approximation, $k^3 \gg k^{-1}$ ($B \ll 1$). With this approximation, Eq. 4 in the low concentration limit ($a/K_1 \ll 1$ and $A > 2$) can be written as:

$$G^0 \approx \tfrac{1}{4}(F^2/RT)ak^{-1}/(a + K_1/2). \tag{13}$$

Fitting this equation to the low-concentration experimental data, one can determine the values of K_1, k^{-1}, and k^1:

$$\begin{aligned} K_1 &= 2K_m = 2\,\text{mM} \\ k^{-1} &= 4(RT/F^2)V_m = 2.36 \times 10^{-18}\,\text{mol/s} \\ k^1 &= k^{-1}/K_1 = 11.8 \times 10^{-16}\,\text{liter/s}. \end{aligned} \tag{14}$$

This value for k^1 can be compared with the diffusion limited value (k_d) described by Läuger (1976):

$$k_d = 2\pi r_0 D, \tag{15}$$

where r_0 is the capture radius and D is the free diffusion coefficient. Assuming a value of 1 Å for r_0 and $10^{-5}\,\text{cm}^2/\text{s}$ for D, one finds the $k_d = 6.3 \times 10^{-16}$ liters/s. Considering the approximations involved, this is in good agreement with the experimental value of k^1. This agreement is strong support for thallium being diffusion limited because if transport across the membrane (k^3) were partially rate limiting, then it can be shown from Eq. 4 that k^1 would have to be even larger, which is not likely because it is already at its theoretical maximum (diffusion-limited) value. Additional support for this model is provided by the value of k^1 of 4×10^{-16} liters/s determined directly by Andersen (1978) from the limiting conductance at high voltage.

The most interesting aspect of the thallium conductance is the fact that as the concentration is raised, the conductance does not level off or decrease, as predicted by Eq. 2, but rises to a much higher value. This means that the increase in the bulk solution concentration must increase the rate of unbinding (k^{-1}) from the channel end, which is the rate-limiting step at the lower concentration. The most likely mechanism is the binding of a third ion in the channel. The general state diagram and kinetics for this model are presented in the Appendix. To simplify the discussion, the low (presented above) and high concentration limit will be treated separately. The high concentration limit is defined by the fact that there are at least two ions per channel, and the state diagram is described by:

(III)

$$\begin{tikzcd} P_L^3 \arrow[r, shift right, "k^{-4}"'] \arrow[r, bend right=40, "k^5e^{\psi/2}"'] & P_2 \arrow[l, shift right, "k^4"'] \arrow[r, shift left, "k^4"] & P_R^3. \arrow[l, shift left, "k^{-4}"] \arrow[l, bend left=40, "k^5e^{-\psi/2}"] \end{tikzcd}$$

In the state P_L^3 a third ion (ion 3) binds at the left end, displacing the ion that was at the left end (ion 2) a small distance into the channel, with ion 1 remaining bound at the right end. The rate constants k^4 and k^{-4} are the rate of binding and unbinding of the third ion. The rate constant k^5 is actually the result of several steps, involving the unbinding of ion 1 and the movement of ion 2 across the membrane. As a first approximation, these two steps have been described by a single step. The flux in this limit is equal to:

$$J = k^5(P_L^3 e^{\psi/2} - P_R^3 e^{-\psi/2}). \qquad (16)$$

It will be assumed that $k^5 \ll k^{-4}$ (see below). Solving for the state variables, the conductance at high concentration (in limit of zero-applied voltage) becomes (Appendix, Eq. 8A, $k^5 \ll k^{-4}$):

$$G^0 = \tfrac{1}{2}(F^2/RT)\, ak^5/(a + K_3/2); \qquad K_3 = k^{-4}/k^4. \qquad (17)$$

Fitting this equation to the high concentration experimental data one finds that:

$$\begin{aligned} K_3 &= 2K_m = 160\ \text{mM} \\ k^5 &= 2(RT/F^2)V_m = 26 \times 10^{-18}\ \text{mol/s}. \end{aligned} \qquad (18)$$

If one examines the sequence of steps that are collectively represented by k^5, it can be shown that at very high concentrations, the rate of rebinding of ion 1 will become fast relative to the crossing of the membrane by ion 2, and the conductance will fall. Because there are no experimental data at very high thallium concentrations, this has not been considered further.

It is not surprising that the model can fit the conductance data because there are a number of adjustable parameters. Two approaches will be used to provide additional support for the model. An approach that will be considered in later sections is to test whether the model and the rate constants determined from the conductance data can fit the other experimental data. The approach that will be considered here is to see if the model is compatible with the electrostatic energy calculations.

The first requirement of the model is that the dissociation constant for the third ion should be about 160 mM. The ratio of the dissociation constant for the third ion (K_3) to that of the first ion (K_1) can be obtained from Eq. 5 and a similar expression for K_3:

$$K_3 = \exp(U + E_T - E_2); \quad K_3/K_1 = \exp E_i^3; \quad E_i^3 = E_T - E_2 - E_1, \qquad (19)$$

where E_T is the total energy (including the interaction with the anion, if present) of a channel that contains three cations in some minimum energy configuration, E_2 is the energy with two cations 1 Å from each end (Table I), and E_1 is the energy of a channel that contains one cation 1 Å from the end (Table I). The energy E_T is listed in Table III as a function of the position in the pore of the central cation and the presence or absence of an anion at the pore mouth. The interaction energy E_i^3, when the anion is absent (first row), is 11.63 kT, corresponding to a dissociation constant ratio of about 10^5 or to a value of K_3 of about 200 M (as K_1 is about 2 mM). Obviously, the extra energy required to put the third cation in the pore is much too large to explain the

TABLE III

ELECTROSTATIC ENERGY DATA FOR THALLIUM MODEL

Position				Energy			K_3/K_1
Anion	Cation 1	Cation 2	Cation 3	E_{anion}	E_T	E_i^3	
	Å from left end				kT		
$-\infty$	1	5	1	0	18.68	11.63	1.1×10^5
-2	1	5	1	-3.34	11.14	4.09	60
-2	1	4	1	-3.44	10.72	3.67	40
-2	1	6	1	-3.24	11.59	4.54	94
-2	1	8	1	-3.07	12.36	5.31	202
-2	1	5	∞	-3.09	6.87		
-2	1	8	∞	-2.82	7.31		
-2	1	11	∞	-2.59	7.25		
-2	1	15	∞	-2.30	6.40		
-2	1	20	∞	-1.98	3.95		
-2	1	24	∞	-1.75	0.68		

experimentally observed K_3 of 160 mM, and this calculation suggests that the proposed three-ion mechanism is not tenable. However, this mechanism does become reasonable if the effect of the counter ions is considered. When there are three cations in the channel, with two of the cations close to one end, one would expect to find an anion very close to the channel mouth. The presence of this anion significantly lowers the energy required to place the third ion in the pore. The energy E_T and E_i^3 when an anion is placed in the bulk solution 2 Å from the pore end is listed in Table III (rows 2–5). The energy E_i^3 is now reduced to about 4 kT, and the ratio K_3/K_1 to about 50 (depending on the exact position of ion 2). Thus, with the anion present, one would predict from the electrostatic calculation that K_3 should be about 100 mM (as K_1 = 2 mM), consistent with the experimental value of 160 mM.

The second requirement of the thallium model is that the binding of the third ion at one end increase the rate of unbinding of the ion at the other end (k^{-1}). The rate of unbinding can be approximated by:

$$k^{-1} = \nu \exp(-U^* - E^*), \tag{20}$$

where U^* is the difference in local free energy between the activated and the bound state and E^* is the difference in the electrostatic energy between the two states. As a first approximation, E^* will be approximated by the difference in total electrostatic energy between the completely unbound and bound states. Thus, the rate of unbinding for the case where there is one ion per pore (k_1^{-1}) or three ions per pore (k_3^{-1}) is described by:

$$k_1^{-1} = \nu \exp(-U^* + E_1), \quad k_3^{-1} = \nu \exp(-U^* - E_2^* + E_T). \tag{21}$$

The ratio of the two constants is:

$$k_3^{-1}/k_1^{-1} = \exp(E_T - E_2^* + E_1). \tag{22}$$

In this equation, E_3 is the energy of the pore when cation 3 is at 1 Å, cation 2 is at about 5 Å, cation 1 is at 24 Å, and the anion is at 2 Å (11.14 kT, row 2, Table III); E_2^* is the energy when cation 1 has left the pore and cations 3, 2, and the anion have not moved (6.87 kT, row 6, Table III); and E_1 is the energy when there is one cation in the pore and the anion has left the pore mouth (2.03 kT, row 2, Table I). Substituting these values into Eq. 22, one finds that k_3^{-1} is about 10 times larger than k_1^{-1} or about 24×10^{-18} mol/s. This value is close to the rate-limiting transport step at high thallium concentrations of 26×10^{-18} (k^5, Eq. 18) and suggests that the unbinding is also rate limiting at the higher concentrations. This is also consistent with the above assumption that $k^5 \ll k^{-4}$.

The third requirement of the thallium model is that after cation 1 unbinds and leaves the pore, the movement of cation 2 across the membrane must be fast compared to the movement when there is only one ion in the pore (k^3). The pore energy (E_T) as a function of the position of cation 2 (after cation 1 has left) is shown in the last six rows of Table III. It can be seen that there is essentially no energy barrier to the movement of cation 2 compared with a large barrier (Fig. 1) that influences k^3 when there is only one ion in the membrane. The calculation of the transport rate from the Nernst-Plank equation (Appendix) indicates that removing the energy barrier should increase k^3 by a factor of at least 50, making the transport of ion 2 across the membrane fast compared with the rate of unbinding of cation 1.

These calculations show that the assumptions of the thallium model are at least consistent with the energy calculations. In addition, the results in Table III provide a simple explanation for another experimental observation. Eisenman et al. (1976) noted that at high thallium concentrations (>5 mM) the anion becomes permeable. This would be predicted from Table III because when there are three thallium ions per channel, the energy of the anion at the channel mouth is about 3.4 kT, which means that the anion concentration at the channel mouth is about 30 times its concentration in the bulk solution. If, for example, the intrinsic anion channel conductance was only 1% of the cation conductance, the effective anion conductance would be 30% at high thallium concentrations when there were three thallium ions in each channel. Also, because the thallium conductance at high concentrations depends on how close the anion can get to the channel mouth, one would predict that the thallium conductance should depend on the anion used.

BI-IONIC POTENTIAL BETWEEN THALLIUM AND POTASSIUM. Eisenman et al. (1976) have measured the potential that results from asymmetric concentrations of thallium and potassium. Their experimental results are summarized in Table IV. In one set of experiments (Table IV, rows 1–3), equal concentrations of TlCl were on the two sides of the membrane and varying amounts of KNO_3 were added to one side; and, in another set (rows 4–6), equal concentrations of KCl were on the two sides, and $TlNO_3$ was added to one side. The permeability ratio was determined from the Goldman equation. There are two critical aspects of these results that must be explained by the model. First, the permeability ratio is altered by thallium concentrations as low as 1 mM and, second, the permeability ratio is relatively independent of the potassium concentration.

TABLE IV

PERMEABILITY RATIO FROM BI-IONIC POTENTIAL FOR Tl^+ AND K^+

Activity (*mM*)				P_{Tl}/P_K	
Side 1		Side 2			
Tl	K	Tl	K	Experimental*	Theoretical‡
0.1	0	0.1	0.1 → 5	4.0	(4.0)
1.0	0	1.0	0.1 → 80	6.3	5.6
10	0	10	3 → 200	13	13.7
0.1	1 → 100	0	1 → 100	3.8	(4.0)
1.0	1 → 100	0	1 → 100	4.5	4.8
10	10 → 100	0	10 → 100	7.0	10

*Eisenman et al., (1976).

‡Eqs. 26 and 29.

Inasmuch as the maximum concentration of thallium used in these studies (10 mM) is much less than the dissociation constant for the third ion (160 mM), it will be assumed that the contribution of the triply occupied channel is negligible. Thus the state diagram (II) is identical to that used for the potassium-sodium bi-ionic potential. The diagram is considerably simplified now because the very high thallium affinity means that the probability of going from P_{ab} (a = thallium, b = potassium) to P_b is much less than the probability of going from P_{ab} to P_a. There is, in effect, a one-way flux from P_b to P_a through P_{ab}. The kinetics have been analyzed in detail in the Appendix, where it is shown that, to a good approximation, the coupling through P_{ab} can be neglected and one can use a set of equations for the flux and permeability ratio that differ from those derived for sodium and potassium (Eqs. 8–10) only because the experimental arrangement of the concentrations was different. To simplify the analysis it will be assumed that terms involving k^2 or K_2 for potassium can be neglected because the maximum potassium concentration used was small compared to K_2 (1,460 mM). It will also be assumed that the thallium is diffusion limited and therefore $k^3 \gg k^{-1}$ for thallium. Then, for the case where $[\mathrm{Tl}]_1 = [\mathrm{Tl}]_2 = a$ and $[K_1] = 0, [K_2] = b$, the potassium flux is described by Eq. 8:

$$J_b = \frac{-bk_b^1k_b^3e^{-\psi/2}}{k_b^{-1} + k_b^3(e^{\psi/2} + e^{-\psi/2})}\,P_0. \tag{23}$$

The thallium flux is equal to (Appendix, Eq. 7A):

$$J_a = \frac{ak_a^3k_a^1(k_a^{-1} + ak_a^2)(e^{\psi/2} - e^{-\psi/2})}{k_a^{-1}[ak_a^2 + k_a^3(e^{\psi/2} + e^{-\psi/2})]}\,P_0. \tag{24}$$

From the bi-ionic condition (Eq. 9), one can solve for exp(ψ), which is in the form of the Goldman equation, and the permeability ratio can be identified (see Eq. 10):

$$\frac{P_a}{P_b} = \left[\frac{k_a^3k_a^1(k_b^{-1} + ak_a^2)}{k_b^1k_b^3k_a^{-1}}\right]\left[\frac{k_b^{-1} + k_b^3(e^{\psi/2} + e^{-\psi/2})}{ak_a^2 + k_a^3(e^{\psi/2} + e^{-\psi/2})}\right]. \tag{25}$$

It can be seen that the permeability ratio is a function of ψ, whereas experimentally it was found to be independent of ψ. However, for the range of ψ that occurred experimentally, the maximum variation with potential would be <20%, probably too small to be observed. In addition, it will be assumed that because the entrance step for the first thallium ion (k^1) is diffusion limited, the entrance of the second thallium ion will be nearly as fast and $k^2 = k^1$. Then, the permeability ratio can be written in the form (zero potential limit):

$$\frac{P_a}{P_b} = \frac{g_a^0(1 + a/K_1^a)}{g_b^0(1 + aB_a/2K_1^a)}; \quad g_a^0 = k_a^1/2;$$

$$g_b^0 = k_b^3 k_b^1/(k_b^{-1} + 2k_b^3); \quad B_a = k_a^{-1}/k_a^3, \tag{26}$$

where g_a^0 and g_b^0 are proportional to the specific conductance in the limit of zero concentration and potential. For the lowest thallium concentration (a) used in Table IV (0.1 mM): $P_a/P_b \simeq g_a^0/g_b^0 = 4$ (because $K_1^a = 2$ mM). Using this result, the theoretical value of P_a/P_b (Eq. 26) is listed in Table IV (rows 1-3), using the previously determined value of K_1^a(2 mM) and a B of 0.30. There is good agreement between theory and experiment. Because $B = k^{-1}/k^3$, a B of 0.3 means that $k^3 = 3.3\ k^{-1}$, and the assumption that was made above that k^{-1} is small compared to k^3 is at least approximately satisfied.

For the case where $[\text{Tl}]_1 = a$, $[\text{Tl}]_2 = 0$, $[\text{K}]_1 = [\text{K}]_2 = b$, the potassium flux is equal to (Appendix, Eq. 7A, assuming terms involving k_b^2 are negligible):

$$J_b = \frac{bk_b^1 k_b^3(e^{\psi/2} - e^{-\psi/2})}{k_b^{-1} + k_b^3(e^{\psi/2} + e^{-\psi/2})} P_0. \tag{27}$$

The thallium flux is described by Eq. 8 (assuming $k_a^3 \gg k_a^{-1}$, and $k_a^2 = k_a^1$):

$$J_a = \frac{ak_a^1 k_a^3(ak_a^1 + 2k_a^{-1})e^{\psi/2}}{ak_a^{-1}k_a^1 + 2k_a^{-1}k_a^3(e^{\psi/2} + e^{-\psi/2})} P_0. \tag{28}$$

And the permeability ratio is (in the limit of zero potential):

$$\frac{P_a}{P_b} = \frac{g_a^0(1 + a/2K_1^a)}{g_b^0(1 + aB/4K_1^a)}. \tag{29}$$

This result for P_a/P_b is listed in Table IV (rows 4–6), using the previously determined values of K_1^a(2 mM), B(0.3), and g_a^0/g_b^0 (4). There is again good agreement between theory and experiment.

As an independent check of the theory, the value of k_a^1 can be determined from the experimental value of g_a^0/g_b^0 (see Eq. 26) and the data determined previously for potassium (Table V):

$$k_a^1 = 2(g_a^0/g_b^0)\, k_b^3 k_b^1/(k_b^{-1} + 2k_b^3) = (8/3)\, k_b^1 = 3.6 \times 10^{-16}\ \text{liters/s}. \tag{30}$$

This value is close to that determined by Andersen (1978) from the limiting conductance (6×10^{-16} liters/s) and about one-third the value determined above from the conductance data (11.8×10^{-16}).

TABLE V

SUMMARY OF CALCULATED VALUES OF CONSTANTS

	Thallium	Potassium	Sodium
K_1, *mm/liter*	2,* 2.5‡	730	700
K_2, *mm/liter*	—	1,460	5,600
K_3, *mm/liter*	160	—	—
k^1, 10^{-16} *liter/s*	11.8,* 6.3,§ 4‖ 3.6¶	1.34,* 1.5‖	1.0
k^{-1}, 10^{-18} *mol/s*	2.36	98	70.
k^3, 10^{-18} *mol/s*	7.87 ($B = 0.3$)	98	35
k^5, 10^{-18} *mol/s*	26	—	—

Each entry corresponds to an independent estimate.

*Conductance data.

‡Inhibition of Na^+ conductance by Tl^+.

§Diffusion limited.

‖Limiting conductance at high voltage.

¶Permeability ratio.

INHIBITION OF SODIUM CONDUCTANCE BY THALLIUM The observation of Neher (1975) that low concentrations of thallium markedly inhibited the sodium conductance provided the first, and still probably the strongest, indication that thallium was different from the other cations. Neher measured the single channel conductance with identical solutions of 2 mM thallium acetate plus varying amounts of sodium acetate on both sides of the membrane. The state diagram is identical to diagram II (which has a very complex general solution). For this case it can be greatly simplified because the contribution of thallium to the total conductance is negligible, and therefore it can be assumed that thallium is at equilibrium. In addition, the state of two sodium ions per channel can be neglected because K_2 for sodium is very large (about 5 M). With these assumptions, the conductance in the zero potential limit is (Appendix, Eq. 22A):

$$G^0 = \frac{(F^2/RT)\, k_c^3\, c/K_1^c}{(1 + 2k_c^3/k_c^{-1})(1 + 2c/K_1^c + 2a/K_1^a + 2ab/K_{ac} + a^2/K_1^a K_2^a)}, \tag{31}$$

where a is the thallium activity, c is the sodium activity, and K_{ac} is the equilibrium dissociation constant for the formation of a channel state that contains one thallium ion and one sodium ion. Inasmuch as K_{ac} should be intermediate between the K_2 for sodium and thallium, it should be relatively large, and this term can also be dropped. The final expression for the conductance can then be written in the form:

$$G = \frac{c\, V_m}{c + K_m + aK_m/K_i} \qquad \begin{aligned} V_m &= \tfrac{1}{2}(F^2/RT)\, k_c^3/(1 + 2k_0^3/k_0^{-1}) \\ K_m &= K_1^c/2 \\ K_i &= K_1^a/(2 + a/K_2^a) \end{aligned} \tag{32}$$

where K_i is the competitive inhibition constant. If it is assumed that K_2^a is large compared to 2 mM, then the K_i of 1.25 mM determined by Neher corresponds to a K_1^a of 2.5 mM (Eq. 32), in good agreement with the value of 2 mM determined above from the conductance data.

DISCUSSION

The major assumption of the model is that the only interaction between ions is electrostatic. Because the channel is formed from only two gramicidin molecules, which must span at least the hydrocarbon region, there will probably be some region of the channel so small that a cation and a water molecule cannot pass each other. Suppose that the well in Fig. 1 is located in this region. Then, for the ion to reach the well, it would have to push the water molecules in the channel ahead of it. When a second ion entered the other end, it would also have to push the water, which would in turn push the ion at the other end out of the binding site. This effect would correspond to a very strong interaction between the ions, making it impossible for two ions to be in the channel at the same time. The most attractive feature of this effect is that it provides a simple explanation for the apparent "high" and "low" affinity components for thallium. The high affinity site would represent the binding of the first ion. As the concentration was raised, the probability would increase that a second ion would enter from the other end, displacing the first ion and increasing the conductance. A kinetic scheme can be derived for this model that quantitatively explains the thallium conductance. The major difficulty with this model is that it cannot explain (although almost every possible kinetic scheme was tried) the two major features of the potassium-thallium bi-ionic potential data: the change in permeability ratio at a concentration of only 1 mM and the fact that the permeability ratio is independent of the potassium concentration.

This emphasizes the importance of examining the bi-ionic data, which is much more difficult to fit than the conductance data, which can be described by many alternative models. The major argument in favor of the model described in this paper is that it provides a simple physical quantitative explanation of the thallium-potassium and sodium-potassium bi-ionic data.

As this strong interaction is not present, the ion must be able to bind to the channel by exchanging with the water at the site and not by pushing the water ahead of it. This implies that the binding sites must be close to the channel mouth. This is what would be predicted from the shape of the electrostatic energy profile in the channel shown in Fig. 1. Because of the steep rise in electrostatic energy at the channel end, the effective minimum in the free energy should be close to the channel mouth even though there may be sites deeper in the channel with a higher intrinsic affinity for the ion. If the model is correct, the decrease in conductance at high concentrations observed for Ce^+, K^+, and NH_4^+ is the result of the binding of the second ion, and the dissociation constant for this binding can be determined from the shape of the conductance curve. For example, the best fit for potassium was obtained for a ratio of K_2/K_1 of about 2, which from the electrostatic energy calculations (Table I) corresponds to a binding position right at the channel mouth. The sodium conductance does not decrease at high concentrations, indicating that the ratio of K_2/K_1 is large (about 8) and that the binding position is somewhat deeper into the channel (about 3 Å, Table I). These values for K_2/K_1 are also consistent with the bi-ionic data for potassium and sodium. The conductance data for Ce^+ and NH_4^+ suggest that they have a binding position similar to that of potassium.

The observation of Neher (1975) that 2 mM thallium could competitively inhibit the sodium conductance indicates that thallium must have a very high affinity in the gramicidin channel. This is confirmed by the conductance measurements of Eisenman et al. (1976). The problem then is to explain the increase in conductance seen with concentrations in the molar range. The most probable explanation is that a third ion binds to the channel at high concentrations, perturbing the binding of the other ions and increasing the conductance. It is shown that this model is compatible with the electrostatic energy calculations if the presence of an anion is included. The conductance measurements of Eisenman et al. (1976) suggest that K^+ (but not Na^+ or Rb^+) also has a high affinity component. However, if the model presented in this paper is correct, it becomes very difficult to explain other experimental results if potassium has a high affinity component. For example, the thallium-potassium bi-ionic permeability ratio should become a function of the potassium activity when it reaches concentrations of the same magnitude as the dissociation constant of the high affinity site. However, experimentally, the permeability ratio is independent of potassium concentrations as high as 300 mM. Similarly, the potassium-sodium bi-ionic potential should show a potassium dependence at much lower concentrations than is observed experimentally if there were a high affinity site. Because the evidence for a high affinity site is not compelling and the experiments are difficult (requiring single channel measurements of very low conductance), it has been assumed in this paper that potassium does not have a high affinity component.

The depth of the well in Fig. 1 can be estimated from the experimental values of the dissociation constant (K). If it is assumed that the bulk solution is equivalent to an ideal lattice gas in which each site is occupied by either an ion or a water molecule and that when an ion is absorbed in the well it displaces a single water molecule, then (Everett, 1964):

$$F = \ln x_i^c x_w^L / x_i^L x_w^c, \tag{33}$$

where F is the free energy (kT) of the binding reaction (or the depth of the well) and x_i^L, x_w^L, x_i^c, and x_w^c are the equilibrium mole fractions of the ion (i) and water (w) in the bulk solution (L) and at the channel binding site (c). When the ionic concentration is equal to the dissociation constant (K), the mole fractions of the ion and water at the binding site are both equal to 1/2, so that:

$$F = \ln K/55. \tag{34}$$

The dissociation constant for potassium and sodium (about 0.7 M) corresponds (Eq. 34) to a well depth of about 4.4 kT. This is about the same size as the energy barrier between the wells and is consistent with the derived result that the rate of crossing the energy barrier in the center of the membrane (k^3) is approximately equal to the rate of going from the well to the bulk solution (k^{-1}) for potassium and sodium. The dissociation constant for thallium (0.002 M) corresponds to a well depth of about 10 kT, much larger than the barrier in the center of the membrane. This is consistent with the conclusion that the rate-limiting step at low thallium concentrations is the movement from the well to the bulk solution (k^{-1}). Although Eq. 33 is a very rough approximation, this analysis shows that the model results are at least consistent with the free energy calculations.

Given the assumption that the only interaction is electrostatic, it becomes difficult to avoid the conclusion that the channel kinetics should exhibit at least the general features of the model presented here. Because of the shape of the electrostatic energy profile, there will be wells at the channel ends, and because the interaction between the wells is small, there will be at least doubly-occupied channels. The kinetics presented here should describe the basic features of a multiply-occupied channel. To keep the kinetics tractable and to limit the number of adjustable parameters, it has been assumed that the entrance steps do not depend on the applied voltage. This assumption is consistent with the conclusion that the wells are close to the channel mouth so that the potential drop between the bulk solution and the well is small. However, there should be some potential dependence, especially for sodium, which may be bound further into the channel and at high potentials when there is a significant voltage drop in the bulk solution (Läuger, 1976). It will probably become necessary to include this potential dependence when more detailed experimental data are available. However, the model presdented here does describe all of the general features observed for the gramicidin channel and should provide at least a step toward a physical model of ionic channels.

APPENDIX

Derivation of Kinetic Equations

The general state diagram for thallium is a combination of the low (I) and high (III) state diagrams in the text:

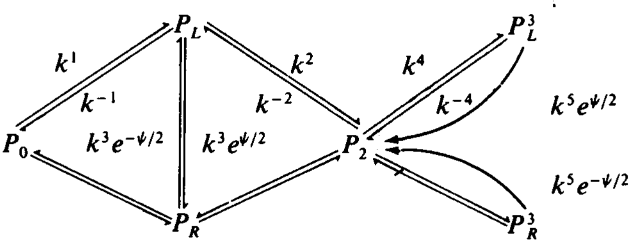

(AI)

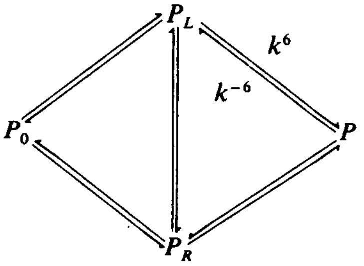

(AI') $P = P_2 + P_L^3 + P_R^3$

Diagram *AI'* is identical to *AI*, but has been reduced to a simpler pattern. The solution to the probability of being in the different states was obtained by the King-Altman procedure (Segal, 1975):

$$\begin{aligned}
DP_L &= a_1k^1k^{-6}[k^6(a_1+a_2)+2k^{-1}]+2k^1k^3k^{-6}(a_1+a_2)e^{-\psi/2}\\
DP_R &= a_2k^1k^{-6}[k^6(a_1+a_2)+2k^{-1}]+2k^1k^3k^{-6}(a_1+a_2)e^{\psi/2}\\
DP_0 &= k^{-1}k^6k^{-6}(a_1+a_2)+2k^{-6}k^3k^{-1}(e^{\psi/2}+e^{-\psi/2})+2k^{-6}(k^{-1})^2\\
DP &= a_1a_2k^1k^6[2k^{-1}+k^6(a_1+a_2)]+k^1k^3k^6[a_1^2e^{\psi/2}\\
&\quad +a_2^2e^{-\psi/2}+a_1a_2(e^{\psi/2}+e^{-\psi/2})] \qquad (1A)\\
D &= DP_L+DP_R+DP_0+DP\\
k^6 &= k^2,\ k^{-6}=k^{-2}/\alpha\\
\alpha &= \frac{(k^{-4}+k^5e^{-\psi/2})(k^{-4}+k^5e^{\psi/2})+ak^4[2k^{-1}+k^5(e^{-\psi/2}+e^{\psi/2})]}{(k^{-4}+k^5e^{-\psi/2})(k^{-4}+k^5e^{\psi/2})}.
\end{aligned}$$

The solute flux (J) through the channel is described by:

$$DJ = k^3[DP_Le^{\psi/2}-DP_Re^{-\psi/2}]+k^5[DP_L^3e^{\psi/2}-DP_R^3e^{-\psi/2}]. \qquad (2A)$$

The states P_L^3 and P_R^3 can be related to the state P:

$$DJ = k^3[DP_Le^{\psi/2}-DP_Re^{-\psi/2}]+\frac{k^5k^4[k^{-4}(a_1e^{\psi/2}-a_2e^{-\psi/2})+k^5(a_1-a_2)]}{\alpha(k^{-4}+k^5e^{\psi/2})(k^{-4}+k^5e^{-\psi/2})}DP. \qquad (3A)$$

Eqs. 1A and 3A provide the complete general solution for the flux (or conductance) when there is only one type of ion present.

CASE I: $a_1 = a_2 = a$ The flux can now be written in the simplified form:

$$D = 2[k^{-1}+k^3(e^{\psi/2}+e^{\psi/2})+ak^6][k^{-1}k^{-6}+2ak^1k^{-6}+a^2k^1k^6] \qquad (4A)$$

$$\begin{aligned}
DJ/(e^{\psi/2}-e^{-\psi/2}) &= 2ak^3k^1k^{-6}(k^{-1}+ak^6)\\
&\quad +\frac{2a^3k^5k^4k^{-4}k^1k^6[k^{-1}+ak^6+k^3(e^{\psi/2}+e^{-\psi/2})]}{\alpha(k^{-4}+k^5e^{\psi/2})(k^{-4}+k^5e^{-\psi/2})}. \qquad (5A)
\end{aligned}$$

Two different limits of Eq. 5A were used in the text. For sodium and potassium (and low concentrations of thallium), there is a maximum of two ions per (diagram I in text) channel, so that the second term in Eq. 5A becomes negligible relative to the first and $ak^4/k^{-1} \ll 1$, so that $k^{-6} = k^{-2}$ and $k^6 = k^2$. In this limit Eq. 5A reduces to:

$$DJ/(e^{\psi/2}-e^{-\psi/2}) = 2ak^3k^1k^{-2}(k^{-1}+ak^2). \qquad (6A)$$

Eq. 4A for D is unchanged except that "6" is replaced by "2." In the bi-ionic potential case it is useful to express J in terms of P_0. This is done by solving DP_0 (Eq. 1A) for D and then substituting into Eq. 6A:

$$J = \frac{ak^3k^1(k^{-1} + ak^2)}{k^{-1}[ak^2 + k^{-1} + k^3(e^{\psi/2} + e^{-\psi/2})]}P_0. \tag{7A}$$

For the other limit of Eq. 5A, the (thallium) concentration is so high that it can be assumed that there are always at least two ions per channel (diagram III in text). In this case, the first term in Eq. 5A becomes negligible relative to the second, $ak^6 \gg k^{-1} \simeq k^{-6}$ and the flux equation reduces to:

$$J = \frac{ak^5k^4k^{-4}}{(k^{-4} + k^5e^{-\psi/2})(k^{-4} + k^5e^{\psi/2}) + ak^4[2k^{-4} + k^5(e^{-\psi/2} + e^{\psi/2})]}. \tag{8A}$$

CASE II: $a_1 = a$, $a_2 = 0$ For this case the solution is needed only for the low concentration limit:

$$DJ = ak^1k^{-2}k^3(2k^{-1} + ak^2)e^{\psi/2} \tag{9A}$$

$$DP_0 = ak^{-1}k^2k^{-2} + 2k^{-2}k^3k^{-1}(e^{\psi/2} + e^{-\psi/2}) + 2k^{-2}(k^{-1})^2. \tag{10A}$$

The solute flux as a function of P_0 is then obtained by solving Eq. 10A for D and substituting into Eq. 9A:

$$J = \frac{ak^1k^3(2k^{-1} + ak^2)e^{\psi/2}}{k^{-1}[ak^2 + 2k^{-1} + 2k^3(e^{\psi/2} + e^{-\psi/2})}P_0. \tag{11A}$$

BI-IONIC POTENTIAL BETWEEN POTASSIUM AND THALLIUM When both potassium and thallium are present, the state is described by diagram II of the text. As discussed in the text, because of the high thallium affinity, there is nearly a one-way flux from potassium to thallium through P_{ab} or P_{ba}. In addition, the potassium concentration is low enough that the state with two potassium ions per channel can be neglected. Finally, only the case when $a_1 = a_2 = a$ and $b_1 = b$, $b_2 = 0$ will be considered (a = thallium activity, b = potassium activity). With these assumptions, the potassium half of diagram II can be written as:

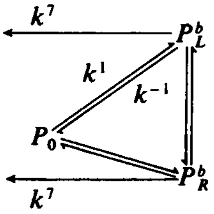

(AII)

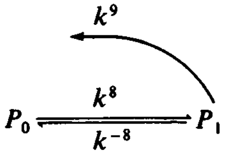

(AII′)

Diagram AII′ is identical to AII if the following identification is made:

$$P_1 = P^b_L + P^b_R$$

$$k^8 = bk^1,\ k^{-8} = k^{-1},\ k^9 = ak^7. \tag{12A}$$

Solving for P^b_L:

$$P^L_b = \frac{b_1k^1 + k^{-3}k^8(k^{-8} + k^9)}{k^{-1} + k^3(e^{\psi/2} + e^{-\psi/2}) + k^9}P_0. \tag{13A}$$

The potassium flux is described by:

$$J_b = bk^1P_0 - P_b^L(k^{-1} + ak^7). \tag{14A}$$

Substituting Eqs. 12A and 13A into Eq. 14A:

$$J_b = \frac{bk^1k^3e^{\psi/2}}{k^{-1} + ak^7 + k^3(e^{\psi/2} + e^{-\psi/2})} P_0. \tag{15A}$$

The constant k^7, the rate that thallium binds to a pore that already contains a potassium ion, is less than the rate of thallium binding to the empty channel (k_a^1). Because the maximum thallium concentration used is 10 mM:

$$ak^7 < 0.01\ k_a^1 = 12 \times 10^{-18}\ \mathrm{mol/s} \ll k^{-1} = 98 \times 10^{-18}. \tag{16A}$$

Thus, the k^7 term in Eq. 15A can be dropped:

$$J_b = \frac{bk^1k^3e^{\psi/2}}{k^{-1} + k^3(e^{\psi/2} + e^{-\psi/2})} P_0. \tag{17A}$$

Eq. 17A is identical to the low concentration limit of the expression obtained above when only a single ion was present (Eq. 11A) and states P_{ab} and P_{ba} were absent.

The thallium half of diagram II is described by:

(AIII)

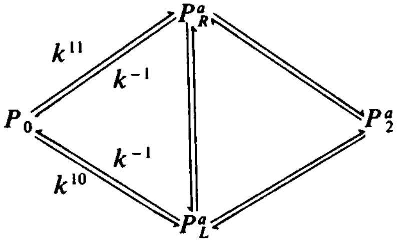

This is identical to diagram I of the text except that k^1P_0 is replaced by:

$$\begin{aligned} k^{10}P_0 &= k^1P_0 + k^7P_R^b \\ k^{11}P_0 &= k^1P_0 + k^7P_L^b. \end{aligned} \tag{18A}$$

The magnitude of the extra factor that results from the presence of states P_{ab} and P_{ba} (k^7 term) can be estimated from Eqs. 13A, 16A, and the fact that $k^{-1} = k^3$ for potassium:

$$k^7P_R^b < k^7P_L^b < k^1P_L^b \simeq k^1P_0b/K_b. \tag{19A}$$

Because K_b is about 700 mM whereas the maximum concentration of potassium (b) used is only about 200 mM, the second term in Eq. 18A is small relative to the first. Thus one can neglect the presence of the states P_{ab} and P_{ba} and assume that potassium and thallium are coupled only through the state P_0.

INHIBITION OF SODIUM CONDUCTANCE BY THALLIUM Diagram II is now simplified because the thallium flux is negligible so that it can be assumed that thallium is at equilibrium, and also the state P_2^c can be neglected because K_2^c is much larger than the sodium concentrations used (a = thallium, c = sodium):

(AIV)

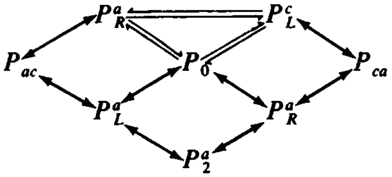

where the double headed arrow indicates equilibrium. The probability of being in the different thallium states is now:

$$P^a_L = P^a_R = aP_0/K^a_1;\quad P^a_2 = a^2P_0/K^a_1K^a_2;\quad P_{ac} = P_{ca} = acP_0/K_{ac}. \qquad (20A)$$

The sodium flux is still described by Eq. 6A but now D has changed to (in the zero potential limit):

$$\begin{aligned} D &= DP^c_L + DP^c_R + DP_0 + 2DP^a_L + 2DP_{ac} + DP^a_2 \\ &= 2k_c^{-2}k_c^{-1}(k_c^{-1} + 2k^3_c)(1 + 2c/K^c_1 + 2a/K^a_1 + 2ac/K_{ac} + a^2/K^a_1K^a_2) \qquad (21A) \end{aligned}$$

By substituting Eq. 21A into Eq. 6A, the final expression for the sodium flux (which is very close to the total flux) is obtained:

$$J = \frac{ck^3_c/K^c_1}{(1 + 2k^3_c/k_c^{-1})(1 + 2c/K^c_1 + 2a/K^a_1 + 2ac/K_{ac} + a^2/K^a_1K^a_2)}. \qquad (22A)$$

Derivation of Kinetic Equations from Nernst-Planck Equation (Equilibrium at the Channel Ends)

It is assumed that the probability of finding an ion in the well is in equilibrium with the bulk solution so that the state probabilities are given by (for the case where $a_1 = a_2 = a$):

$$P_L = P_R = P_0a/K_1,\; P_2 = P_0a^2/K_1K_2$$

$$P_0 + 2P_L + P_2 = 1 \rightarrow P_0 = (1 + 2a/K_1 + a^2/K_1K_2)^{-1}. \qquad (23A)$$

The solute flux can be derived from the Nernst-Planck equation following the procedure used in the first paper (Levitt, 1978):

$$J = -D[P_{mR}\exp(\psi_{mR} + E_{mR} + U_{mR}) - P_{mL}\exp(\psi_{mL} + E_{mL} + U_{mL})]/\int_{x_1}^{x_2}\exp(\psi + E + U)\mathrm{d}x, \qquad (24A)$$

where D is the diffusion coefficient in the pore; P_{mL} and P_{mR} are the probabilities of finding an ion in the left or right well (regardless of whether the opposite well is occupied); ψ, E, and U are the electrical potential, the total electrostatic energy, and local free energy when the ion is in the well (subscript mR or mL) or at position x (no subscript). The integration goes from the left well (x_1) to the right well (x_2). The energy E is a function of concentration because it is the total energy and therefore depends on the number of ions in the channel, which depends on the bulk concentration. Eq. 24A is of the same form as Eq. 1, and the rate constant for crossing the membrane (k^3) can be identified (in the limit $\psi \ll 1$):

$$k^3(a) = D/\int P_m\mathrm{d}x/P(x);\quad P_m/P_x = \exp(E + U - E_m - U_m), \qquad (25A)$$

where k^3 has been expressed in terms of the ratio of the equilibrium probability of finding an ion at x ($P(x)$) relative to that of finding it in the well (P_m). In a multiply occupied channel, E, and therefore k^3, is a function of concentration. $P(x)$ is equal to the sum of the probability of having a channel that contains just one ion located at x (P_1) plus a channel that contains two ions, one at x and the other either in the left (P_{2L}) or right (P_{2R}) well:

$$P(x) = P_1(x) + P_{2L}(x) + P_{LR}(x) = P_1(x)[1 + a/K_2(x) + a/K_2(d - x)]$$

$$P_m = P_{1m}(1 + a/K_2);\; P_1(x) = P_{1m} \exp [U_{1m} + E_{1m} - U_1(x) - E_1(x)], \qquad (26A)$$

where $K_2(x)$ and K_2 are the dissociation constants for the reaction of an ion going from the well to the bulk solution when there is another ion at x or in the opposite well, respectively; d is the pore length and the subscript "1" indicates the case when there is just one ion in the pore. By substituting Eq. 26A into Eq. 25A, the general expression for k^3 is obtained:

$$k^3(a) = D[(1 + a/K_2) \int_{x_1}^{x_2}$$

$$\exp (U_{1m} + E_{1m} - U_1(x) - E_1(x))/(1 + a/K_2(x) + a/K_2(d - x))]^{-1} \qquad (27A)$$

The integral is dominated by values at the peak of barrier ($x = d/2$) and from the electrostatic energy calculations it can be shown that $a/K_2(d/2) \ll 1$ (for most concentrations) and therefore k^3 can be approximated by:

$$k^3(a) \simeq k^3(0)/(1 + a/K_2). \qquad (28A)$$

where $k^3(0)$ is the rate of crossing the membrane if there is at most one ion per channel. Also, from Eq. 23A:

$$P_{mL} = P_{mR} = P_L + P_2 = (a/K_1)(1 + a/K_2)/(1 + 2a/K_1 + a^2/K_1K_2). \qquad (29A)$$

The final expression for the solute flux (Eqs. 1, 28A, and 29A) is:.

$$J/\psi = k^3(0)(a/K_1)/(1 + 2a/K_1 + a^2/K_1K_2). \qquad (30A)$$

The result derived in the text (see Eq. 4) reduces to Eq. 30A if the rate of leaving the channel (k^{-1}) is much larger than the rate of crossing the membrane (k^3). This is equivalent to the assumption of equilibrium at the ends.

The permeability ratio for the case where $a_1 = a$, $a_2 = 0$, $b_1 = 0$, and $b_2 = b$ can be determined from the solute flux equations when two different ions are present (see Eq. 24A):

$$J_a = D_a P^a_{mL} \exp (U^a_{mL} + E^a_{mL})/\int \exp (\psi + E^a + U^a)\mathrm{d}x$$

$$J_b = -D_b P^b_{mR} \exp (U^b_{mR} + E^b_{mR} + \psi_d)/\int \exp (\psi + E^b + U^b)\,\mathrm{d}x. \qquad (31A)$$

The energy E^a or E^b is the total energy of a channel that contains an a or b ion at position x and may or may not contain another ion ending (of either type) in one of the wells, depending on the concentration in the bulk solution. Because there is equilibrium at the ends:

$$P^a_{mL} \exp (U^a_{mL} + E^a_{mL}) = a;\quad P^b_{mR} \exp (U^b_{mR} + E^b{}_{mR}) = b. \qquad (32A)$$

The integral is dominated by values in the center of the membrane where U should be nearly constant ($U(d/2)$) so that J_a (or J_b) can be written as:

$$J_a = aD_a \exp(-U_a(d/2))/\int \exp(\psi + E^a). \qquad (33A)$$

The expression for ψ_d is then obtained from Eqs. 31A–33A and the bi-ionic condition (Eq. 9):

$$\exp(\psi_d) = P_a/P_b = \frac{D_a \exp(-U_a(d/2))/\int \exp(\psi + E^b)}{D_b \exp(-U_b(d/2))/\int \exp(\psi + E^a)}. \qquad (34A)$$

Because the electrostatic energy depends only on the charge of the ion $E^a(x) = E^b(x)$ and:

$$P_a/P_b = \frac{D_a \exp(-U_a(d/2))}{D_b \exp(-U_b(d/2))}. \qquad (35A)$$

Because it has been assumed that all the interaction between ions is electrostatic, the local potential U is not a function of the number of ions in the channel and therefore the permeability ratio is a constant, independent of concentration.

I wish to thank Dr. George Eisenman, Dr. Olaf Andersen, and Dr. Steven Hladky for sending me preprints of their papers.

This research was supported by grants from the Minnesota Medical Foundation and the University of Minnesota Computer Center.

Received for publication 29 July 1977 and in revised form 21 December 1977.

REFERENCES

ANDERSON, O. S. 1978. Ion transport across simple membranes. *In* Renal Function. G. H. Giebisch and E. Purcell, editors. Independent Publisher Group, Port Washington, N.Y. In press.

CHIZMADJEV, YU. A., and S. KH. AITYAN. 1977. Ion transport across sodium channels in biological membranes. *J. Theor. Biol.* **64**:429–453.

EISENMAN, G., J. SANDBLOM, and E. NEHER. 1976. Ionic selectivity, saturation, binding, and block in the gramicidin A channel: a preliminary report. *In* Metal-Ligand Interactions in Organic Chemistry and Biochemistry. B. Pullman and N. Goldblum, editors. D. Reidel Publishing Co., Dordrecht-Holland.

EVERETT, D. H. 1964. Thermodynamics of adsorption from solution. *Trans. Faraday Soc.* **60**:1803–1813.

HECKMANN, K., B. LINDEMANN, and J. SCHNAKENBERG. 1972. Current-voltage curves of porous membranes in the presence of pore-blocking ions. *Biophys. J.* **12**:683–702.

HILLE, B. 1975*a*. Ionic selectivity, saturation, and block in sodium channels: a four-barrier model. *J. Gen. Physiol.* **66**:535–560.

HILLE, B. 1975*b*. Ionic selectivity of Na and K channels of nerve membranes. *In* Membranes. Vol. 3. G. Eisenman, editor. Marcel Dekker, Inc., New York. 255–324.

HLADKY, S. B., and D. A. HAYDON. 1972. Ion transfer across lipid membranes in the presence of gramicidin A. I. Studies of the unit conductance channel. *Biochim. Biophys. Acta.* **274**:294–312.

HLADKY, S. B. 1974. Pore or carrier? Gramicidin A as a simple pore. *In* Drugs and Transport Processes. B. A. Callingham, editor. University Park Press, Baltimore.

HLADKY, S. B., B. W. URBAN, and D. A. HAYDON. 1978. *In* Ion Permeation through Membrane Channels. C. F. Stevens and R. W. Tsien, editors. Raven Press, New York. In press.

LAÜGER, P. 1973. Ion transport through pores: a rate-theory analysis. *Biochim. Biophys. Acta.* **311**:423–441.

LAÜGER, P. 1976. Diffusion-limited ion flow through pores. *Biochim. Biophys. Acta.* **455**:493–509.

LEVITT, D. G. 1978. Electrostatic calculations for an ion channel. I. Energy and potential profiles and interactions between ions. *Biophys. J.* **22**:209–219.

MYERS, B. V., and D. A. HAYDON. 1972. Ion transfer across lipid membranes in the presence of gramicidin A. II. The ion selectivity. *Biochim. Biophys. Acta.* **274**:313–322.

NEHER, E. 1975. Ionic specificity of the gramicidin channel and the thallous ion. *Biochim. Biophys. Acta.* **401**:540–544.

SANDBLOM, J., G. EISENMAN, and E. NEHER. 1977. Ionic selectivity, saturation and block in gramicidin A channels. I. Theory for the electrical properties of ion selective channels having two pairs of binding sites and multiple conductance states. *J. Membr. Biol.* **31**:383–417.

SEGAL, I. H. 1975. Enzyme Kinetics. John Wiley & Sons Inc., New York.